Acta Crystallographica Section D
Biological Crystallography
ISSN 0907-4449

Structural analysis of the positive AMPA receptor modulators CX516 and Me-CX516 in complex with the GluA2 ligand-binding domain

Christian Krintel,[a] Kasper Harpsøe,[a]‡ Linda G. Zachariassen,[a] Dan Peters,[b]§ Karla Frydenvang,[a] Darryl S. Pickering,[a] Michael Gajhede[a] and Jette S. Kastrup[a]*

[a]Department of Drug Design and Pharmacology, Faculty of Health and Medical Sciences, University of Copenhagen, Universitetsparken 2, DK-2100 Copenhagen, Denmark, and [b]NeuroSearch A/S, Pederstrupvej 93, DK-2750 Ballerup, Denmark

‡ Present address: The Novo Nordisk Foundation Center for Protein Research, Faculty of Health and Medical Sciences, University of Copenhagen, Blegdamsvej 3B, DK-2200 Copenhagen, Denmark.
§ Present address: DanPET AB, Rosenstigen 7, 21619 Malmö, Sweden and Aniona ApS, Pederstrupsvej 93, 2750 Ballerup, Denmark.

Correspondence e-mail: jsk@sund.ku.dk

Received 8 February 2013
Accepted 30 April 2013

PDB References: GluA2 ligand-binding domain, complex with CX516, 4iy5; complex with Me-CX516, 4iy6

Positive allosteric modulators of the ionotropic glutamate receptor A2 (GluA2) can serve as lead compounds for the development of cognitive enhancers. Several benzamide-type (*S*)-2-amino-3-(3-hydroxy-5-methyl-4-isoxazolyl)propionic acid (AMPA) receptor modulators such as aniracetam, CX516 and CX614 have been shown to inhibit the deactivation of AMPA receptors with a less pronounced effect on desensitization. Despite CX516 being an extensively investigated AMPA receptor modulator and one of the few clinically evaluated compounds, the binding mode of CX516 to AMPA receptors has not been reported. Here, the structures of a GluA2 ligand-binding domain mutant in complex with CX516 and the 3-methylpiperidine analogue of CX516 (Me-CX516) are reported. The structures show that the binding modes of CX516 and Me-CX516 are similar to those of aniracetam and CX614 and that there is limited space for substitution at the piperidine ring of CX516. The results therefore support that CX516, like aniracetam and CX614, modulates deactivation of AMPA receptors.

1. Introduction

The (*S*)-2-amino-3-(3-hydroxy-5-methyl-4-isoxazolyl)propionic acid (AMPA) receptors, comprising subunits GluA1–4, are tetrameric glutamate-gated ion channels. The AMPA receptors mediate postsynaptic fast excitatory signalling in the mammalian brain and have been investigated as a drug target in cognitive disorders such as Alzheimer's disease (Bowie, 2008). Each of the individual AMPA receptor subunits is composed of an extracellular N-terminal domain, a ligand-binding domain (LBD), a transmembrane domain and an intracellular C-terminal domain (Sobolevsky *et al.*, 2009). The LBD contains two subdomains, D1 and D2, that are connected *via* an interdomain hinge region. In the tetrameric receptor the LBDs are arranged as a 'dimer of dimers', with the dimer interface composed of two neighbouring D1 subdomains (Sobolevsky *et al.*, 2009). Upon glutamate binding the D2 subdomain reorients around glutamate and the LBD adopts a 'closed clam-shell-like' agonist-bound form, placing a conformational strain on the transmembrane segments that leads to opening of the ion-channel pore (Armstrong & Gouaux, 2000). Two distinct processes lead to ion-channel closure (Arai & Kessler, 2007; Jin *et al.*, 2005; Sun *et al.*, 2002). Desensitization involves a rearrangement of the D1–D1 dimer interface, causing the channel to close with the LBD in its agonist-bound form. Deactivation involves removal of the agonist, leading the LBD to return to its unbound state and the ion channel to close.

Positive allosteric modulators of AMPA receptors act by attenuating either deactivation or desensitization or both processes (Jin *et al.*, 2005; Sun *et al.*, 2002). CX516 (BDP-12, BA-74, Ampalex) is one of the earliest developed cognitive enhancers acting on AMPA receptors (ampakines) following the discovery of the potentiation of AMPA-evoked currents by aniracetam (Fig. 1; Ito *et al.*, 1990). Even though relatively high potencies have been reported for aniracetam from experiments on isolated AMPA receptors, studies performed on AMPA receptors in hippocampal slices indicated that CX516 is more potent than the earlier compound aniracetam (Arai *et al.*, 1996; Suppiramaniam *et al.*, 2001; Tang *et al.*, 1991). Although later discontinued, CX516 was one of the first ampakines to enter human trials and was shown to improve cognitive performance in schizophrenic, elderly and healthy subjects (Goff *et al.*, 2001; Ingvar *et al.*, 1997; Lynch *et al.*, 1997). CX516 is not nearly as potent as subsequently developed benzamide ampakines such as CX614, but it remains one of the most investigated cognitive enhancers and is still widely used within research (Broberg *et al.*, 2009; Damgaard *et al.*, 2010). A number of studies have shown that the action of CX516 and other benzamide ampakines such as aniracetam, CX546 and CX614 can be attributed to their ability to slow deactivation (Arai & Lynch, 1998), while benzothiadiazine dioxides such as cyclothiazide, IDRA-21 and diazoxide primarily reduce desensitization (Yamada & Rothman, 1992; Yamada & Tang, 1993). A structural interpretation of the latter scenario has, with the cocrystal structures of cyclothiazide and IDRA-21 in complex with the GluA2 LBD, shown that benzothiadiazine dioxide modulators attenuate desensitization by stabilizing the D1–D1 dimer interface (Ptak *et al.*, 2009; Sun *et al.*, 2002). A stabilization of the D1–D1 interface can also be accomplished by the L483Y mutation. This mutation blocks receptor desensitization (Stern-Bach *et al.*, 1998) and renders the isolated LBD dimeric in solution without altering the modulator-binding pocket (Krintel *et al.*, 2012; Sun *et al.*, 2002). Furthermore, cocrystal structures of CX614 and aniracetam indicated that stabilization of the agonist-bound form leads to inhibition of deactivation by the benzamide type of modulators (Jin *et al.*, 2005).

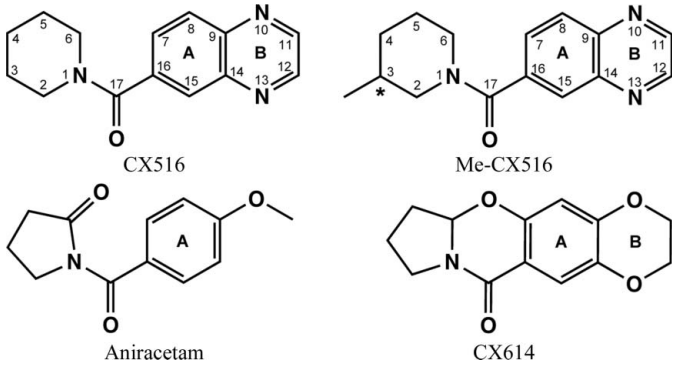

Figure 1
Chemical structures of the AMPA receptor modulators CX516, Me-CX516, aniracetam and CX614. The chiral centre of Me-CX516 is denoted by an asterisk. The ring systems are denoted A and B.

AMPA receptors exist in kinetically distinct 'flip' and 'flop' isoforms arising from alternative splicing (Mosbacher *et al.*, 1994; Sommer *et al.*, 1990) and several modulators preferentially potentiate either of these isoforms. A key amino acid located at the D1–D1 dimer interface varies between the two splice forms: *i.e.* Ser754 (flip) and Asn754 (flop) (numbering without signal peptide). Whereas modulators such as cyclothiazide and IDRA-21 show a preference for the flip isoform owing to a steric clash with Asn754, aniracetam, CX516 and CX614 seem to have a slight preference for the flop isoform (Arai & Kessler, 2007; Arai *et al.*, 2000; Partin *et al.*, 1996).

Even though CX516 is a well studied compound, a structural investigation of CX516 has so far not been reported. As part of a drug-discovery programme at NeuroSearch A/S, analogues of CX516 were designed and synthesized with an emphasis on alterations of the piperidine-ring structure. The 3-methyl-substituted piperidine (Me-CX516) was shown to potentiate currents from human GluA1 with a similar potency as the parent compound CX516 (Peters *et al.*, 2007). The observation that Me-CX516 possesses activity as an AMPA receptor modulator indicated that there was room for substitution in the piperidine ring. To further evaluate the possibility of substitution at the piperidine ring, we employed X-ray crystallography on a soluble construct of the ligand-binding domain of GluA2.

2. Materials and methods

2.1. Modulators

CX516 and Me-CX516 were synthesized as described in the Supplementary Material.[1]

2.2. Two-electrode voltage-clamp electrophysiology

The rat GluA2(Q)$_i$ (natural RNA-edited Ca^{2+}-permeable variant of the ionotropic glutamate receptor A2 flip isoform with a glutamine at position 586; numbering without signal peptide) isoform clone in the vector pIRES-BlasAN was used for the preparation of cRNA transcripts for functional expression in *Xenopus laevis* oocytes (White *et al.*, 2002). cRNA was synthesized using the AmpliCap-Max T7 High Yield Message Maker transcription kit (Cellscript Inc., Madison, Wisconsin, USA).

X. laevis oocytes were obtained and prepared as previously detailed (Greenwood *et al.*, 2006). Recordings were made at room temperature at a holding potential of −60 mV while the oocytes were continuously superfused with Ca^{2+}-free frog Ringer's solution (115 mM NaCl, 2 mM KCl, 1.8 mM $BaCl_2$, 5 mM HEPES pH 7.0). CX516 and Me-CX516 were dissolved in DMSO as 300 mM stock solutions, which were stored at 243 K and were freshly diluted into Ca^{2+}-free frog Ringer's solution. All dilutions were adjusted to contain 1%(v/v) DMSO (final concentration). (S)-Glutamate (10 mM) was freshly prepared from 500 mM frozen stock solutions. CX516

[1] Supplementary material has been deposited in the IUCr electronic archive (Reference: KW5064). Services for accessing this material are described at the back of the journal.

Table 1
X-ray data-collection and refinement statistics.

Values in parentheses are for the outer resolution bin.

	GluA2 LBD-L483Y-N754S–CX516	GluA2 LBD-L483Y-N754S–(*R*)-Me-CX516
PDB entry	4iy5	4iy6
X-ray source	Synchrotron radiation	Synchrotron radiation
Wavelength (Å)	1.0	1.0
Space group	$P2_12_12$	$P2_12_12$
Unit-cell parameters (Å)	a = 99.08, b = 121.69, c = 47.30	a = 64.33, b = 101.04, c = 47.36
Resolution (Å)	26.43–2.00 (2.11–2.00)	23.7–1.72 (1.82–1.72)
Unique reflections	39394 (5687)	33234 (4350)
Completeness (%)	99.8 (100.0)	98.4 (89.8)
Average multiplicity	5.2 (5.2)	4.7 (4.5)
$\langle I/\sigma(I)\rangle$	5.2 (2.1)	7.8 (5.6)
$R_{\rm merge}$†	0.104 (0.313)	0.053 (0.126)
Wilson B (Å^2)	16.1	16.4
Refinement		
$R_{\rm work}$‡	0.153	0.135
$R_{\rm free}$§	0.200	0.168
No. of residues		
Molecule *A*	263	263
Molecule *B*	263	—
No. of modulators	2	3
No. of (*S*)-glutamates	2	1
No. of waters	572	386
No. of glycerols	3	1
No. of sulfates	5	2
No. of chlorides	3	—
R.m.s.d. from ideal¶		
Bond lengths (Å)	0.007	0.010
Bond angles (°)	1.0	1.2
Mean B factors (Å^2)		
Molecule *A*	15.5	15.6
Molecule *B*	18.0	—
Water	26.7	27.8
Glycerol	45.5	36.6
Sulfate	46.2	41.0
Chloride	55.6	—
Modulator (*A*/*B*/*C*/*D*††)	15.5/15.2/—/—	9.3/—/33.2/32.0
(*S*)-Glutamate (*A*/*B*)	8.4/10.4	8.1/—
Ramachandran plot‡‡		
Outliers (%)	0	0
Favoured (%)	99.1	98.9
Rotamer outliers‡‡ (%)	1.8	0.9
C^β outliers‡‡ (%)	0	0
Clashscore‡‡	4.2	4.9

† A measure of agreement among multiple measurements of the same reflections. $R_{\rm merge}$ is calculated as $\sum_{hkl}\sum_i |I_i(hkl) - \langle I(hkl)\rangle|/\sum_{hkl}\sum_i I_i(hkl)$, where $I_i(hkl)$ is the intensity of an individual measurement of the reflection with Miller indices hkl and $\langle I(hkl)\rangle$ is the average intensity from multiple observations. ‡ $R_{\rm work} = \sum_{hkl}||F_{\rm obs}| - |F_{\rm calc}||/\sum_{hkl}|F_{\rm obs}|$, where $F_{\rm obs}$ and $F_{\rm calc}$ are the observed and calculated structure-factor amplitudes, respectively. § The free R factor, $R_{\rm free}$, is computed in the same manner as $R_{\rm work}$ but using only a small set (5%) of randomly chosen intensities that were not used in the refinement of the model. ¶ Ideal bond lengths and angles were taken from Engh & Huber (1991). †† *A* and *B* (each with half occupancy) denote modulator molecules bound in the modulator-binding pocket. *C* and *D* denote modulator molecules bound at the protein surface. ‡‡ *MolProbity* statistics (Chen *et al.*, 2010).

and Me-CX516 were co-applied with 10 m*M* (*S*)-glutamate and were added by batch application until a plateau response was obtained. The potentiation at each concentration of CX516 and Me-CX516 was calculated as the percentage increase relative to the control current [10 m*M* (*S*)-glutamate + 1%(*v*/*v*) DMSO].

Repeated-measures ANOVA (RM-ANOVA) with a Holm–Sidak post-test was used for statistical comparison of responses, which were considered to be significantly different if $P < 0.05$. For graphical representation of data, responses were pooled from all experiments and normalized to the control response at each individual oocyte.

2.3. Protein preparation and crystallization

The structure of the flop isoform of the GluA2 LBD, first published by Armstrong & Gouaux (2000), has an asparagine present at position 754. However, for our GluA2 modulator studies we used GluA2 LBD-L483Y-N754S [the LBD construct of GluA2 with a serine at position 754 resembling the dimer interface of the flip isoform and a tyrosine at position 483 (numbering without signal peptide) rendering the LBD construct dimeric in solution; Krintel *et al.*, 2012]. The N754S mutation provides a dimer interface resembling that of the flip isoform and allows the accommodation of a wider variety of compounds owing to a slightly larger modulator-binding pocket. The construct also has the L483Y mutation which renders the protein dimeric in solution and thus creates a preformed modulator-binding pocket (Krintel *et al.*, 2012). In the study of Krintel *et al.* (2012), we demonstrated that a similar dimer was formed by GluA2 LBD-N754S and GluA2 LBD-L483Y-N754S. Furthermore, we showed that CTZ binds in an identical manner in GluA2 LBD-N754S and LBD-L483Y-N754S. The rat GluA2 LBD-L483Y-N754S mutant protein was expressed and purified as described previously (Krintel *et al.*, 2012).

Cocrystallization was performed at 279 K by the hanging-drop vapour-diffusion method. The drops consisted of 1 µl protein solution and 1 µl crystallization solution. The protein solution consisted of 6 mg ml^{-1} GluA2 LBD-L483Y-N754S in 10 m*M* HEPES pH 7.0, 20 m*M* NaCl, 1 m*M* EDTA, 1 m*M* (*S*)-glutamate. For cocrystallization experiments, 0.5–1 mg of either CX516 or Me-CX516 was added to 150 µl protein solution and incubated for 72 h prior to crystallization. This leads to saturating concentrations of the modulators. The crystallization conditions were 24.4%(*w*/*v*) PEG 4000, 0.3 *M* lithium sulfate, 0.1 *M* phosphate–citrate pH 4.5 for the CX516 complex and 15.2%(*w*/*v*) PEG 4000, 0.3 *M* lithium sulfate, 0.1 *M* sodium acetate pH 5.5 for the Me-CX516 complex. The crystals were soaked in crystallization solution containing 20%(*w*/*v*) glycerol and flash-cooled in liquid nitrogen.

2.4. Data collection, structure determination and refinement

X-ray diffraction data were collected on beamline I911-2 at MAX-lab, Lund, Sweden. The GluA2 LBD-L483Y-N754S–CX516 and GluA2 LBD-L483Y-N754S–Me-CX516 data sets were scaled and indexed using *iMosflm* and *SCALA* within *CCP*4 (Battye *et al.*, 2011; Winn *et al.*, 2011). The structures were solved by molecular replacement using *Phaser* (McCoy *et al.*, 2007) with the GluA2 LBD-L483Y-N754S structure (PDB entry 3tdj, molecule *A*; Krintel *et al.*, 2012) as the search model. *ARP*/*wARP* (Langer *et al.*, 2008) was used for initial model building. Water molecules were added by *ARP*/*wARP* and then deleted before modelling of the modulator. Various electron-density maps, including those from the *Phaser* solution without water molecules, were consulted during refine-

ments. Further model building was performed in *Coot* (Emsley & Cowtan, 2004). Refinements were performed using *PHENIX* (Adams *et al.*, 2010). For the GluA2 LBD-L483Y-N754S–CX516 structure the model was refined using translation–libration–screw motion (TLS) and isotropic *B* factors. For the GluA2 LBD-L483Y-N754S–Me-CX516 structure the model was initially refined using isotropic *B* factors and in later stages of refinement using riding H atoms and isotropic *B* factors.

CX516 and Me-CX516 were built using *Maestro* (v.9.2; Schrödinger). To obtain low-energy conformations, the two modulators were subjected to a conformational search in *MacroModel* (v.9.9; Schrödinger) using the MMFFs force field at default settings. At least ten lowest energy conformations for each ligand were then evaluated in comparison to the electron-density maps.

The quality of the structures was validated using tools in *Coot* (Emsley & Cowtan, 2004) and *MolProbity* (Chen *et al.*, 2010). For data and refinement statistics, see Table 1.

Domain closures were calculated using *DynDom* (Hayward & Berendsen, 1998). Figures were prepared using *PyMOL* (v.1.5.0.1; Schrödinger).

3. Results

3.1. Potentiation of GluA2 currents by CX516 and Me-CX516

Preparations of CX516 and racemic Me-CX516 were tested for their ability to potentiate rat GluA2$(Q)_i$ expressed in *X. laevis* oocytes by two-electrode voltage-clamp (TEVC) electrophysiology. In these tests the 3 m*M* responses for each compound were statistically significantly different from the control responses, while the potentiations by CX516 and Me-CX516 at each concentration were not statistically significantly different (Fig. 2).

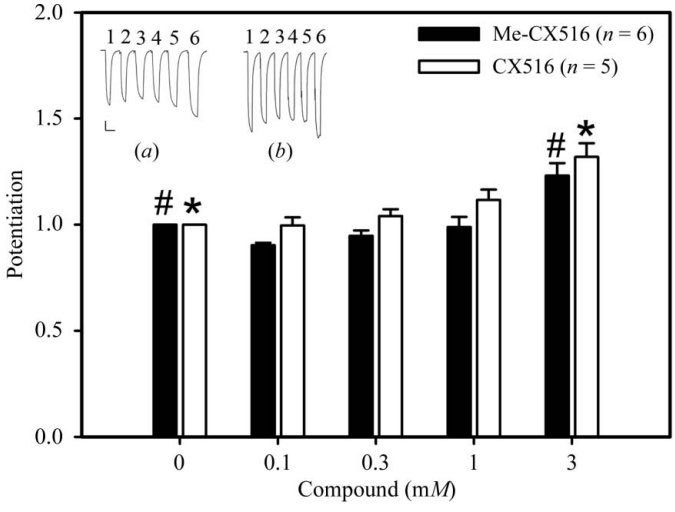

Figure 2
Normalized potentiation of glutamate responses at GluA2$(Q)_i$ receptors expressed in *X. laevis* oocytes and recorded by two-electrode voltage-clamp electrophysiology. Only the 3 m*M* potentiator concentrations gave responses that were statistically different from the control responses. The asterisks and hashes indicate responses that are statistically significantly different from control responses [10 m*M* (*S*)-glutamate in 1% DMSO]: $P < 0.05$, one-way RM-ANOVA with Holm–Sidak post-test. Inset, current traces from two oocytes: (*a*) Me-CX516, (*b*) CX516. All stimulations used 10 m*M* (*S*)-glutamate. 1, glutamate alone; 2, plus 1%(*v*/*v*) DMSO; 3, plus 0.1 m*M* compound; 4, plus 0.3 m*M* compound; 5, plus 1 m*M* compound; 6, plus 3 m*M* compound. Scale bars: 500 nA, 100 s. $V_h = -60$ mV.

3.2. Structure of GluA2 LBD in complex with CX516

The rat GluA2 LBD mutant (LBD-L483Y-N754S, which is predominantly in a dimeric form in solution; Krintel *et al.*, 2012) was used for crystallization experiments. GluA2 in complex with CX516 and glutamate crystallized as a dimer with two subunits in the asymmetric unit of the crystal. CX516 is bound at the D1–D1 interface (Fig. 3) in the region in which binding of aniracetam also occurs. CX516 is located on a noncrystallographic twofold axis, leading to the modelling of two CX516 molecules each with an occupancy of 0.5. Electron-density maps of CX516 are shown in Fig. 4(*a*) and Supplementary Fig. S1. Data-collection and refinement statistics can be found in Table 1.

3.3. Structure of GluA2 LBD in complex with Me-CX516

GluA2 LBD-L483Y-N754S in complex with Me-CX516 and glutamate also crystallized as a dimer (Supplementary Fig. S2) but with a single subunit in the asymmetric unit of the crystal. Thus, the dimer is formed by crystallographic twofold symmetry. As racemic Me-CX516 was used for crystallization, both the (*R*)- and (*S*)-enantiomers were modelled individually at the dimer interface. However, a low-energy conformation could only be fitted to the electron density for the (*R*)-enantiomer, with the methyl group in an equatorial position. Hence, the final model contains the (*R*)-enantiomer and in this case the modulator is located on the crystallographic twofold axis, leading to the modelling of one (*R*)-Me-CX516 molecule with the occupancy set to 0.5. Electron-density maps of

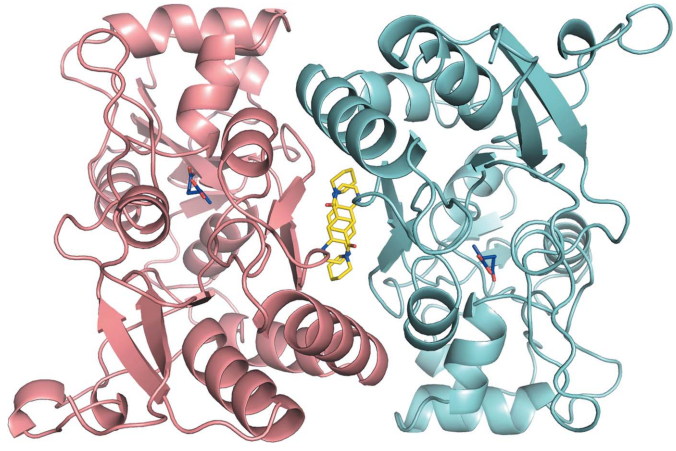

Figure 3
CX516 (yellow stick representation) binds at the dimer interface of GluA2 LBD-L483Y-N754S in two different orientations and (*S*)-glutamate (blue stick representation) binds at the agonist-binding site. The protein molecules are shown as salmon (molecule *A*) and cyan (molecule *B*) cartoon representations.

Me-CX516 are shown in Fig. 4(*b*) and Supplementary Fig. S1. Data-collection and refinement statistics are given in Table 1.

Weak electron densities corresponding to two extra Me-CX516 molecules, in addition to the molecule bound at the dimer interface, were found (Supplementary Fig. S2). One Me-CX516 molecule was located near Lys506 and Lys697 (additional site 1) and one molecule was located near Thr643 and Tyr673 (additional site 2), both with an occupancy of 0.8 after refinement. These two additional Me-CX516 molecules line the protein surface. In additional site 1 stacking is observed between the bicyclic ring system of Me-CX516 and Tyr469 of a symmetry-related molecule. In additional site 2 Me-CX516 forms a potential hydrogen bond from one N atom in the bicyclic ring system to the side-chain $N^{\varepsilon 2}$ atom of a symmetry-related His412. In the structure with CX516 it was not possible to locate CX516 at the additional sites, which might be a consequence of the lower resolution of this structure, as crystal packing would allow binding of CX516 in these sites. We regard the presence of these Me-CX516 molecules to be a consequence of saturating Me-CX516 concentrations; however, a functional role cannot be ruled out.

3.4. Comparison of GluA2 LBD structures with CX516 and Me-CX516

Binding of glutamate in the agonist-binding site and CX516 at the dimer interface of GluA2 LBD leads to a closure of subdomain D2 towards D1 of 20.3° and 21.9° for the *A* and *B* molecules, respectively, compared with the apo structure of GluA2 (PDB entry 1fto, molecule *A*; Armstrong & Gouaux, 2000). The closure of D2 towards D1 in the complex with glutamate and Me-CX516 bound is 20.4°. These values are similar to those observed for GluA2 LBD-L483Y-N754S in complex with glutamate and cyclothiazide (21.3–22.1°; Krintel *et al.*, 2012). The domain closure of glutamate alone in GluA2 LBD varies from 19.1° to 21.3° (Pøhlsgaard *et al.*, 2011) and is therefore comparable to the domain closures observed in the presence of CX516 and Me-CX516.

Both CX516 and Me-CX516 form a hydrogen bond between the carbonyl O atom and one water molecule (W1; Fig. 5*a*). Through W1, CX516 and Me-CX516 are connected to a network of water molecules (W2, W3 and W4) held in place by Ile481 and Gly731 of one subunit and Pro494 and Ser754 of the second subunit (numbering without signal peptide). In both CX516 and Me-CX516 the N10 nitrogen forms a hydrogen bond to water molecule W5, which further makes hydrogen bonds to Ser729 and Lys730. Ser729 also forms a hydrogen bond to another water molecule, W6, which makes a hydrogen bond to Ser497 of the opposite subunit. Thereby, a water-mediated bridge is created across the dimer interface.

The aromatic ring systems of CX516 and Me-CX516 have numerous nonpolar interactions across the dimer interface, primarily to Pro494, Phe495, Met496 and Ser497 of one subunit and to Ser729, Lys730 and Gly731 of the opposite subunit. Also, the piperidine ring makes nonpolar interactions primarily with Ser729 and Lys730 of one subunit and with Phe495 and Met496 of the opposite subunit (Fig. 5*b*). The piperidine ring of Me-CX516 is positioned similarly to that of CX516 and the 3-methyl substituent reaches towards Leu758, thereby providing extra nonpolar interactions of Me-CX516.

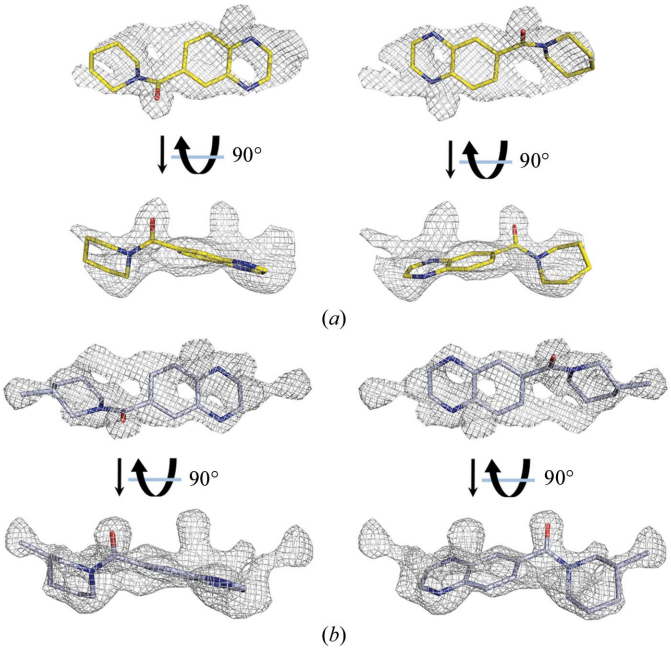

Figure 4
OMIT $F_o - F_c$ electron-density maps for CX516 (*a*) and (*R*)-Me-CX516 (*b*). For clarity, only one conformation is fitted at a time and two views 90° apart are shown. In (*a*) the map is contoured at the 2.5σ level (0.29 e Å^{-3}) and in (*b*) at the 3σ level (0.36 e Å^{-3}).

4. Discussion

CX516 and racemic Me-CX516 were synthesized and tested for their ability to potentiate glutamate-evoked currents at rat GluA2(Q)$_i$ and we found both to weakly potentiate currents at ∼3 m*M* concentrations. This is in contrast to previously published results (Arai *et al.*, 1996), in which field recordings on rat hippocampal slices showed significant increases in steady-state currents recorded at a concentration of 1 m*M* CX516. However, the observations presented here are based on recombinant homomeric GluA2(Q)$_i$ expressed in *X. laevis* oocytes and recorded by TEVC. Native AMPA receptors in hippocampal slices are associated with accessory proteins (*e.g.* stargazin) which modify their pharmacology and can increase the observed potency of positive allosteric modulators (Tomita *et al.*, 2006). We did not co-express any accessory proteins along with GluA2(Q)$_i$ and therefore our results are not directly comparable to those at native AMPA receptors. It was not possible to determine the EC_{50} values of either compound owing to solubility limitations. Hence, we could not employ saturating concentrations of these compounds to measure the maximum potentiations, but there was no difference in the potency of CX516 and Me-CX516 at the tested concentrations (Fig. 2). However, since Me-CX516 is a racemic mixture, a variation in potency of the two enantiomers cannot be ruled out and it is therefore possible that the potency of the (*R*)-enantiomer of Me-CX516 is equal to or

higher than that of CX516. This would be in agreement with the observation that only (*R*)-Me-CX516 fits the observed electron density in the GluA2 LBD structure.

Preliminary isothermal titration calorimetry experiments were also conducted with GluA2 LBD-L483Y-N754S in the presence of 5 m*M* glutamate and increasing concentrations of aniracetam, CX516 or Me-CX516. However, owing to a very low enthalpy of binding or a very weak binding affinity it was not possible to determine the binding constants (results not shown).

CX516 has previously been shown to modulate deactivation of receptors with a less pronounced effect on desensitization, as also observed for CX614 and aniracetam (Arai *et al.*, 1996, 2000; Tang *et al.*, 1991). Several features of the binding mode of CX516 and Me-CX516 reported here support these results, as the binding modes of CX516 and Me-CX516 are very similar to those of aniracetam and CX614 (Jin *et al.*, 2005). Firstly, an overlay of the CX614 and aniracetam GluA2 LBD complex structures with that of CX516 shows that the orientation of the carbonyl O atom is conserved, with rings A and B matching almost perfectly (Fig. 1 and Fig. 6*a*). In all three structures the carbonyl O atom connects the modulators to a network of four water molecules, W1, W2, W3 and W4, held in place by amino acids from both LBD subunits of the dimeric GluA2 (Fig. 6*a*). Also, the contact of the N10 atom of both CX516 and Me-CX516, forming a hydrogen bond to a water molecule (W5), is observed in the structures with aniracetam and CX614 (which have ether O atoms instead of N atoms). W5 in addition makes a hydrogen bond to Ser729 and thus mediates an indirect contact between the modulator and Ser729. Secondly, the W6 water-mediated contact between Ser729 and Ser497 of the opposite subunit is also observed in the CX614 and aniracetam structures. Therefore, this water-mediated contact is central to the binding mode of benzamidine modulators. As previously observed for aniracetam and CX614 (Jin *et al.*, 2005), the side chain of Ser497 also reorients in the structures with CX516 and Me-CX516 in order for the receptor to accommodate the modulator compared with Ser497 in the GluA2 apo structure (Armstrong & Gouaux, 2000). Taken together, the contacts to the D1–D2 interdomain hinge are conserved among the structures. However, Ser729 was modelled in two conformations in the structure with Me-CX516, whereas Ser729 was located in two conformations only in one molecule of the dimer in the structure with CX516. In

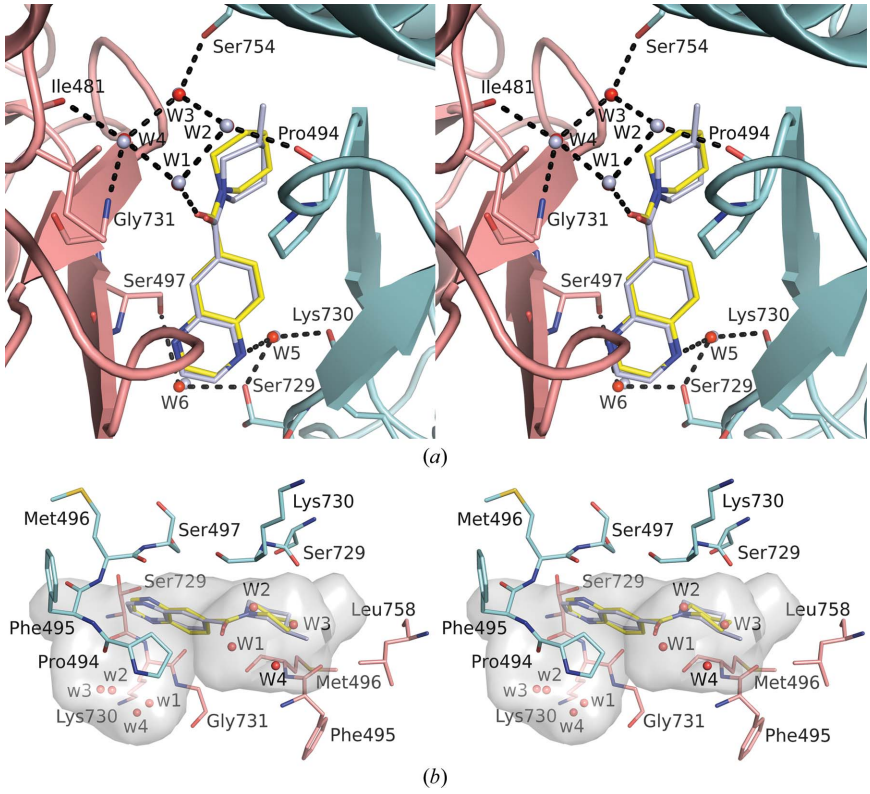

Figure 5
Stereoview of GluA2 binding-site interactions of CX516 and (*R*)-Me-CX516. (*a*) Potential hydrogen bonds to CX516 (yellow stick representation) and (*R*)-Me-CX516 (light blue stick representation) are shown as dashed lines. Key residues from the complex with CX516 are shown in stick representation and labelled. Water molecules W1–W6 are shown as red and light blue spheres for the CX516 and (*R*)-Me-CX516 complexes, respectively. For clarity, only protein molecules *A* (cyan cartoon representation) and *B* (salmon cartoon representation) of GluA2 LBD-L483Y-N754S with CX516 bound are shown. (*b*) Nonpolar interaction partners of CX516 and (*R*)-Me-CX516. Key residues and water molecules W1–W4 from the complex with CX516 are shown in stick representation and as red spheres, respectively (w1–w4 correspond to W1–W4 but form contacts to CX516 when it is in the opposite orientation). The primary nonpolar interaction partners of the aromatic ring systems are Pro494, Phe495, Met496 and Ser497 (shown in cyan) and Ser729, Lys730 and Gly731 (shown in salmon). Primary nonpolar interaction partners of the piperidine rings are Ser729 and Lys730 (shown in cyan) and Phe495 and Met496 (shown in salmon). The 3-methyl substituent of (*R*)-Me-CX516 makes nonpolar interactions with Leu758 (shown in salmon). A contour of the modulator-binding pocket is shown in grey.

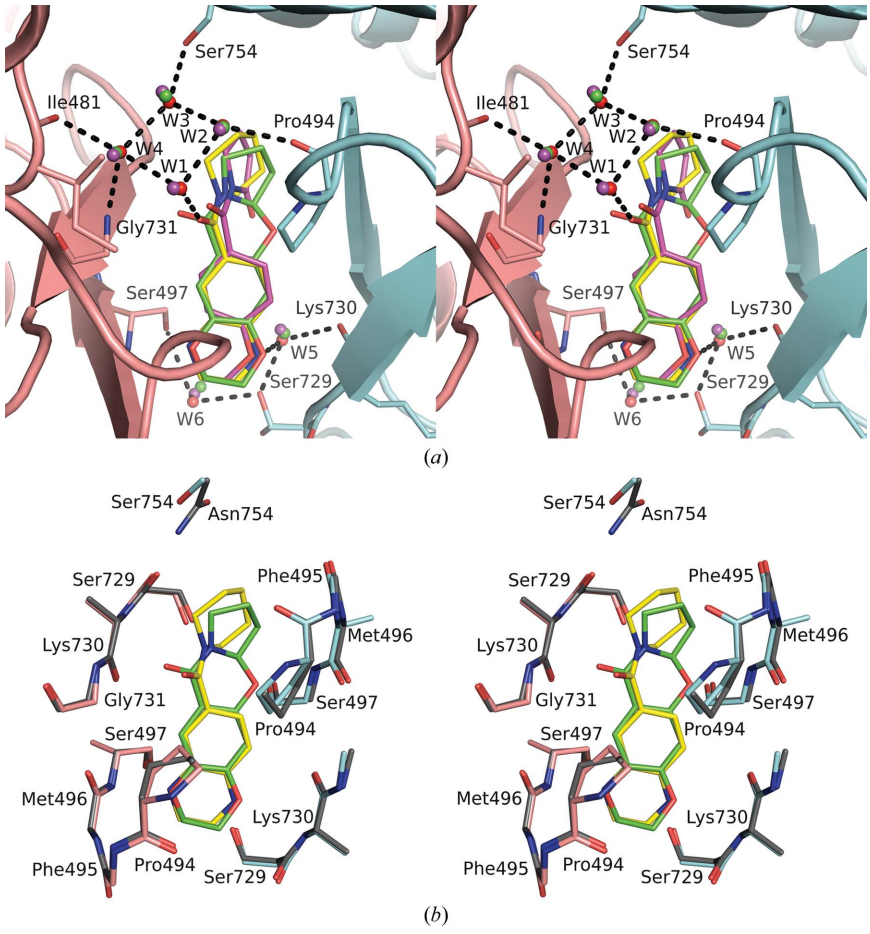

Figure 6
Comparison of CX516, aniracetam and CX614 binding modes in GluA2 shown in stereoview. (*a*) Overlay of the structures of CX516 (yellow) bound to GluA2 LBD-L483Y-N754S and aniracetam (magenta) and CX614 (green) bound to GluA2 LBD (PDB entries 2al5 and 2al4, respectively). Ordered water molecules (W1–W6) are shown as red, magenta and green spheres for the CX516, aniracetam and CX614 complexes, respectively. For clarity, only protein molecules *A* (cyan cartoon representation) and *B* (salmon cartoon representation) of GluA2 LBD-L483Y-N754S with CX516 bound are shown. (*b*) Overlay of CX516 (yellow) bound to GluA2 LBD-L483Y-N754S (cyan and salmon) and CX614 (green) bound to GluA2 LBD (grey). Residues within a 5 Å distance of the modulators are shown. It should be noted that only part of the side chain is shown for some residues.

the structures with aniracetam and CX614 only one conformation was built. It has previously been speculated by Jin *et al.* (2005) that the structural mechanisms of receptor desensitization and deactivation could be conceptually separable. It was suggested that stabilization of the dimer interface primarily affects receptor desensitization, whereas stabilization of the closed-clamshell state of the ligand-binding domain slows deactivation. Since CX516 and Me-CX516, as well as aniracetam and CX614, bind to the D1–D2 hinge-region residues (Ser497, Ser729, Lys730 and Gly731), it is likely that the modulation of deactivation occurs by stabilization of the closed-clamshell conformation. On the other hand, binding of CX516 and Me-CX516 also contributes to the stabilization of the D1–D1 interface, thereby slowing desensitization.

CX516 has previously been shown to potentiate AMPA receptors with a potency lower than that of CX614 but higher than that of aniracetam (Arai *et al.*, 1996, 2000; Suppiramaniam *et al.*, 2001; Tang *et al.*, 1991). The binding modes of CX516 and Me-CX516 support these results. CX614 is a larger and more rigid molecule compared with CX516 and aniracetam, enabling extensive van der Waals interactions with the two protein subunits of the LBD dimer and a lower entropy loss during binding. In turn, CX516 is larger and more rigid than aniracetam, supporting a potency of CX516 between those of aniracetam and CX614.

It has previously been reported that CX516 shows a small preference for the flop isoforms of AMPA receptors (Arai & Kessler, 2007). The structure of CX516 presented here is in complex with a GluA2 LBD mutant containing a serine at position 754 as observed in the flip isoform of GluA2. Overlaying this structure with that of CX614 in complex with the flop GluA2 LBD (PDB entry 2al4; Jin *et al.*, 2005) shows only minor differences in the binding pocket (Fig. 6*b*). In both structures the hydrogen bond connecting W3 to the LBD is conserved when replacing Asn754 (flop) by Ser754 (flip) (Fig. 6*a*). Thus, it seems likely that the binding mode of CX516 will be similar in the flip and flop isoforms of GluA2 LBD. Therefore, the structure of CX516 does not explain the higher preference of CX516 for the flop isoform. As the flip/flop region extends from the LBD to the linker region connecting

to the transmembrane part, residues outside the modulator-binding site might be responsible for this difference.

Based on the structures of GluA2 LBD in complex with CX516 and Me-CX516, an analysis of possible substitution patterns at the piperidine ring was performed. Introduction of a methyl group at the 3-position of the piperidine ring of CX516 does not result in any overall or local changes in the dimer interface of GluA2. However, the positions of CX516 and Me-CX516 in the modulator-binding pocket reveal a limited space for substitutions at the piperidine ring except for substitutions pointing towards the space occupied by W1–W4 (Fig. 5*b*). For example, substituents at the 2-position can reach this area. However, even small substituents might lead to an unfavourable displacement of W1–W4 if not replaced by favourable contacts to the LBD. Studies at NeuroSearch A/S have confirmed that substitution at the 2-position hampers modulator potency and the only CX516 analogue other than Me-CX516 found to potentiate human GluA1 at the level of CX516 was the azepane analogue (data not shown).

We acknowledge the technical assistance of Jørgen Bach Pedersen, Tove Thomsen, Gitte Friberg and Heidi Peterson. We would also like to thank Max-lab, Lund, Sweden for providing beamtime. This work was supported by GluTarget and Danscatt.

References

Adams, P. D. *et al.* (2010). *Acta Cryst.* D**66**, 213–221.
Arai, A. C. & Kessler, M. (2007). *Curr. Drug Targets*, **8**, 583–602.
Arai, A., Kessler, M., Rogers, G. & Lynch, G. (1996). *J. Pharmacol. Exp. Ther.* **278**, 627–638.
Arai, A. C., Kessler, M., Rogers, G. & Lynch, G. (2000). *Mol. Pharmacol.* **58**, 802–813.
Arai, A. & Lynch, G. (1998). *Brain Res.* **799**, 230–234.
Armstrong, N. & Gouaux, E. (2000). *Neuron*, **28**, 165–181.
Battye, T. G. G., Kontogiannis, L., Johnson, O., Powell, H. R. & Leslie, A. G. W. (2011). *Acta Cryst.* D**67**, 271–281.
Bowie, D. (2008). *CNS Neurol. Disord. Drug Targets*, **7**, 129–143.
Broberg, B. V., Glenthøj, B. Y., Dias, R., Larsen, D. B. & Olsen, C. K. (2009). *Psychopharmacology*, **206**, 631–640.
Chen, V. B., Arendall, W. B., Headd, J. J., Keedy, D. A., Immormino, R. M., Kapral, G. J., Murray, L. W., Richardson, J. S. & Richardson, D. C. (2010). *Acta Cryst.* D**66**, 12–21.
Damgaard, T., Larsen, D. B., Hansen, S. L., Grayson, B., Neill, J. C. & Plath, N. (2010). *Behav. Brain Res.* **207**, 144–150.
Emsley, P. & Cowtan, K. (2004). *Acta Cryst.* D**60**, 2126–2132.
Engh, R. A. & Huber, R. (1991). *Acta Cryst.* A**47**, 392–400.
Goff, D. C., Leahy, L., Berman, I., Posever, T., Herz, L., Leon, A. C., Johnson, S. A. & Lynch, G. (2001). *J. Clin. Psychopharmacol.* **21**, 484–487.
Greenwood, J. R., Mewett, K. N., Allan, R. D., Martín, B. O. & Pickering, D. S. (2006). *Neuropharmacology*, **51**, 52–59.
Hayward, S. & Berendsen, H. J. (1998). *Proteins*, **30**, 144–154.
Ingvar, M., Ambros-Ingerson, J., Davis, M., Granger, R., Kessler, M., Rogers, G. A., Schehr, R. S. & Lynch, G. (1997). *Exp. Neurol.* **146**, 553–559.
Ito, I., Tanabe, S., Kohda, A. & Sugiyama, H. (1990). *J. Physiol.* **424**, 533–543.
Jin, R., Clark, S., Weeks, A. M., Dudman, J. T., Gouaux, E. & Partin, K. M. (2005). *J. Neurosci.* **25**, 9027–9036.
Krintel, C., Frydenvang, K., Olsen, L., Kristensen, M. T., de Barrios, O., Naur, P., Francotte, P., Pirotte, B., Gajhede, M. & Kastrup, J. S. (2012). *Biochem. J.* **441**, 173–178.
Langer, G., Cohen, S. X., Lamzin, V. S. & Perrakis, A. (2008). *Nature Protoc.* **3**, 1171–1179.
Lynch, G., Granger, R., Ambros-Ingerson, J., Davis, C. M., Kessler, M. & Schehr, R. (1997). *Exp. Neurol.* **145**, 89–92.
McCoy, A. J., Grosse-Kunstleve, R. W., Adams, P. D., Winn, M. D., Storoni, L. C. & Read, R. J. (2007). *J. Appl. Cryst.* **40**, 658–674.
Mosbacher, J., Schoepfer, R., Monyer, H., Burnashev, N., Seeburg, P. H. & Ruppersberg, J. P. (1994). *Science*, **266**, 1059–1062.
Partin, K. M., Fleck, M. W. & Mayer, M. L. (1996). *J. Neurosci.* **16**, 6634–6647.
Peters, D., Christensen, J. K., Harpsøe, K. & Liljefors, T. (2007). International Patent WO 2007/060144 A2.
Pøhlsgaard, J., Frydenvang, K., Madsen, U. & Kastrup, J. S. (2011). *Neuropharmacology*, **60**, 135–150.
Ptak, C. P., Ahmed, A. H. & Oswald, R. E. (2009). *Biochemistry*, **48**, 8594–8602.
Sobolevsky, A. I., Rosconi, M. P. & Gouaux, E. (2009). *Nature (London)*, **462**, 745–756.
Sommer, B., Keinänen, K., Verdoorn, T. A., Wisden, W., Burnashev, N., Herb, A., Köhler, M., Takagi, T., Sakmann, B. & Seeburg, P. H. (1990). *Science*, **249**, 1580–1585.
Stern-Bach, Y., Russo, S., Neuman, M. & Rosenmund, C. (1998). *Neuron*, **21**, 907–918.
Sun, Y., Olson, R., Horning, M., Armstrong, N., Mayer, M. & Gouaux, E. (2002). *Nature (London)*, **417**, 245–253.
Suppiramaniam, V., Bahr, B. A., Sinnarajah, S., Owens, K., Rogers, G., Yilma, S. & Vodyanoy, V. (2001). *Synapse*, **40**, 154–158.
Tang, C.-M., Shi, Q.-Y., Katchman, A. & Lynch, G. (1991). *Science*, **254**, 288–290.
Tomita, S., Sekiguchi, M., Wada, K., Nicoll, R. A. & Bredt, D. S. (2006). *Proc. Natl Acad. Sci. USA*, **103**, 10064–10067.
White, H. S., Sarup, A., Bolvig, T., Kristensen, A. S., Petersen, G., Nelson, N., Pickering, D. S., Larsson, O. M., Frølund, B., Krogsgaard-Larsen, P. & Schousboe, A. (2002). *J. Pharmacol. Exp. Ther.* **302**, 636–644.
Winn, M. D. *et al.* (2011). *Acta Cryst.* D**67**, 235–242.
Yamada, K. A. & Rothman, S. M. (1992). *J. Physiol.* **458**, 409–423.
Yamada, K. A. & Tang, C.-M. (1993). *J. Neurosci.* **13**, 3904–3915.